



Enhanced adsorption performance of PPy/TiO₂ prepared on surface of TiO₂ without calcination

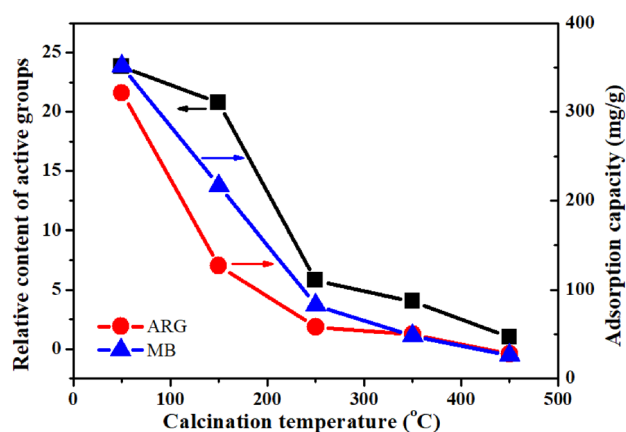
Jingjing Li¹ · Jiangtao Feng² · Wei Yan²

© Springer Nature Switzerland AG 2019

Abstract

The PPy/TiO₂ composites were synthesized by polymerizing pyrrole monomer on the surface of TiO₂ calcined at different temperatures. The results of Fourier Transform Infrared spectroscopy, X-ray diffraction, Temperature programmed desorption, X-ray photoelectron spectroscopy and Zeta potential showed that the type and amount of the active groups on TiO₂ surface decreased with the increase of calcination temperature, leading to a significant decline in its adsorption capacity for Acid Red G (ARG) and Methylene Blue (MB). This also had a significant influence on the physicochemical property and adsorption performance of PPy/TiO₂. The prepared PPy/TiO₂ composite exhibited an enhanced adsorption capacity for ARG and MB. The adsorption ability of PPy/TiO₂ was the strongest when TiO₂ was not calcined and gradually decreased with the increase of the calcination temperature of TiO₂. The PPy/TiO₂ composite without calcination was chosen to investigate its adsorption performance. The results showed that the adsorption behaviors of ARG and MB on PPy/TiO₂ were described by the pseudo-second-order and Langmuir isotherm models with the maximum adsorption amount of 424.75 and 439.61 mg/g for ARG and MB, respectively. Finally, the surface chemical properties of TiO₂ seriously affected the adsorption performance of PPy/TiO₂. The PPy/TiO₂ composite could possess excellent adsorption performance when the selected TiO₂ contained more hydroxyl and carboxyl groups.

Graphical abstract



Keywords TiO₂ · PPy · Composite · Adsorption · Surface chemistry

✉ Jingjing Li, lijingjing21@shu.edu.cn | ¹Materials Genome Institute, Shanghai University, Shanghai 200444, China. ²Department of Environmental Science and Engineering, Xi'an Jiaotong University, Xi'an 710049, Shaanxi, China.



SN Applied Sciences

(2019) 1:617

| <https://doi.org/10.1007/s42452-019-0628-8>

Received: 22 January 2019 / Accepted: 16 May 2019

Published online: 21 May 2019

SN Applied Sciences
A SPRINGER NATURE journal

1 Introduction

Because of the positively charged nitrogen atoms in PPy matrix, PPy can adsorb metal ions, inorganic anions and some organics through ion exchange or electrostatic interaction [1, 12, 22]. However, the application of pure PPy is restricted because pure PPy has low adsorption ability and is difficult to be reused due to its low density.

Some researchers began to synthesize composite materials by combining PPy with other materials to solve these two shortcomings. Bhaumik et al. [2] investigated the adsorption performance of the prepared PPy/Fe₃O₄ composite for Cr(VI), and found that the composite exhibited outstanding adsorption ability with the maximum adsorption amount of 169.4 mg/g. Li et al. [13, 14] synthesized PPy/TiO₂ composites in HNO₃ and H₂SO₄ solutions, respectively, and evaluated their adsorption performances for acid red G and methylene blue. The results showed that the PPy/TiO₂ composites displayed much better adsorption ability than pure PPy [7]. Chen et al. [5] investigated the influence of metal oxides on the adsorption performance of PPy/metal oxides for methylene blue, which suggested that the composites exhibited various adsorption abilities by using different substrate materials. In our previous study, PPy/TiO₂ prepared in different carboxylic acid with hydroxyl group showed different adsorption capacities [8]. However, it did not systematically analyze the effect of the surface physicochemical properties of the substrate materials on the adsorption performance of the formed composites.

In this work, TiO₂ particles prepared in citric acid were calcined in different temperatures to change the physicochemical properties of the surface. The calcined TiO₂ particles were then used as the substrates to synthesize the PPy/TiO₂ composites. The corresponding adsorption capacities for Acid Red G and Methylene Blue were discussed, in order to confirm that the surface physicochemical properties of the substrate materials influenced the adsorption performance of the formed composites.

2 Experimental

2.1 Materials

Pyrrole (98%, Qingquan Pharmaceutical & Chemical Ltd., Zhejiang, China) was distilled twice under reduced pressure, and then stored in the dark under low temperature. Acid Red G (ARG) was commercial grade and purified before used. Methylene Blue (MB), FeCl₃·6H₂O, HNO₃ (65–68%), NaOH, citric acid, n-propanol (99.9%)

and tetrabutyl titanate (TBOT, 98%) were of analytical grade and purchased from Beijing Chemical Reagent Co., China. The deionized water used for all experiments was obtained from the EPED-40TF Superpure Water System (EPED, China).

2.2 Synthesis of adsorbents

The TiO₂ powder was synthesized by hydrolysis method. A mixture of TBOT and n-propanol (the volume ratio is 5:2) was added into 200 mL citric acid solution (65 °C, 0.16 mol/L), with magnetic stirring for 2 h. The suspension was then continuously stirred for 12 h at ambient temperature. Finally, the white solid was filtrated and washed several times with DI water until the pH value of the washing liquid became neutral. The TiO₂ powders were dried at 50 °C for 24 h and named as 50-TiO₂. 50-TiO₂ particles calcined at 150 °C, 250 °C, 350 °C and 450 °C were named as 150-TiO₂, 250-TiO₂, 350-TiO₂ and 450-TiO₂, respectively.

The preparation process of the PPy/TiO₂ composite was described as follows. First, 0.1 g of the calcined TiO₂ was added into 100 mL deionized water by ultrasonic vibrating for 10 min. Then, the mixture was cooled to 5 °C and magnetically stirred for 30 min. Afterwards, pyrrole (0.30 mL) was added into the mixture and stirred for 30 min, followed by adding dropwise FeCl₃ (3.0 mol/L, 4.0 mL) solution in 1 h. The mixture needed 24 h to complete the reaction. Finally, the generated black solid was filtered and washed with deionized water several times, and dried at 50 °C for 24 h. According to the calcination temperature of TiO₂, the prepared PPy/TiO₂ composites were named as 50-PPy/TiO₂, 150-PPy/TiO₂, 250-PPy/TiO₂, 350-PPy/TiO₂ and 450-PPy/TiO₂, respectively.

2.3 Characterizations

The structures of the as-prepared samples were examined by Fourier transform infrared spectra (FT-IR) using the KBr pellet method on a BRUKER TENSOR 37 FT-IR spectrophotometer in the range of 4000–400 cm⁻¹. XRD diffraction was utilized to measure the crystallinity of the samples by X'Pert PRO MRD Diffractometer using Cu-Kα radiation. The surface chemistry characterization of the samples was estimated by temperature programmed desorption (TPD) using Builder Gas Adsorption analyzer PCA-1200 (Beijing, China) in He flow (30.0 mL/min) and at a heating rate of 10 °C/min to 700 °C. The oxidative states of the samples were determined using X-ray photoelectron spectroscopy (XPS) on Kratos Axis Ultra DLD with an Al monochromatic X-ray source (1486.71 eV). All binding energies (BEs) were referenced to the C1s hydrocarbon peak at 284.6 eV. The BET surface area (SBET), total

pore volume (V) and average pore radius (R) were measured at 77 K using Builder SSA-4200 (Beijing, China).

The zeta potentials were measured with Malvern Zeta-sizer Nano ZS90. Samples for zeta potential measurement were prepared by adding 5 mg of sample in 10 mL NaCl solution (10^{-3} mol/L) at different pH values. The pH was adjusted with diluted HNO_3 or NaOH solution.

2.4 Adsorption experiments

The suspension containing 800 mg/L of dye solution and 2 g/L of adsorbent was shook for 120 min at 25 °C. Then the suspension was centrifuged at 4000 rpm for 5 min. The obtained supernatant was analyzed by the UV–Vis spectrophotometer (Agilent 8453) at the wavelength of 506 nm for ARG and 665 nm for MB.

The influences of pH and ionic concentration on the adsorption capacity of PPy/TiO₂ were further studied. The suspension containing 300 mg/L of ARG or MB and 2 g/L PPy/TiO₂ was stirred for 1 h. The pH values of suspensions were adjusted to 1.0–13.0 with NaOH or HNO_3 solution. Then the suspension was centrifuged at 4000 rpm for 5 min. The clarified supernatant was analyzed by the UV–Vis spectrophotometer (Agilent 8453). The effect of ionic concentration (0–0.3 mol/L) on the adsorption was carried out by adding Na_2SO_4 into the 300 mg/L ARG and MB solution.

The adsorption rate R (%) and the amount of dye molecules adsorbed onto adsorbent Q_t (mg/g) after time t were calculated from the following Eqs. (1) and (2), respectively:

$$R(\%) = \frac{C_0 - C_t}{C_0} \times 100 \quad (1)$$

$$Q_t(\text{mg/g}) = \frac{C_0 - C_t}{M} \times V \quad (2)$$

where C_0 is the initial dye concentration (mg/L), and C_t is the concentration of dye after time t ; V is the solution volume (L) and M is the mass of the used adsorbent (g).

The adsorption equilibrium of ARG or MB with different concentrations (300, 500, 800 mg/L) on PPy/TiO₂ was evaluated at 20 °C, with 2 g/L of PPy/TiO₂ added and stirred for 1 h. The mixture was fetched per 10 min and filtered, and then the filtrates were analyzed by the UV–Vis spectrophotometer. The adsorption kinetics were analyzed by using the pseudo-first (Eq. 3) and pseudo-second orders (Eq. 4):

$$\lg(Q_e - Q_t) = \lg Q_e - \frac{k_1}{2.303} t \quad (3)$$

$$\frac{t}{Q_t} = \frac{1}{k_2 Q_e^2} + \frac{t}{Q_e} \quad (4)$$

where t is the contact time (min); k_1 (min^{-1}) and k_2 (g/mg/min) are the rate constants for the pseudo-first-order and pseudo-second-order models, respectively; Q_e (mg/g) is the adsorption amount at equilibrium state.

Equilibrium adsorption isotherms at 20 °C were obtained by mixing different concentrations (300–1000 mg/L) of ARG or MB solutions with 2 g/L of PPy/TiO₂. There are two models, Langmuir and Freundlich isotherms, which are described in the following Eqs. (5) and (6), respectively:

$$Q_e = \frac{Q_{\max} K_L C_e}{1 + K_L C_e} \quad (5)$$

$$Q_e = K_F C_e^{1/n} \quad (6)$$

where Q_{eq} and Q_{\max} (mg/g) are the adsorbed dye equilibrium concentration in the solid phase and the maximum adsorption capacity, respectively; C_{eq} (mg/L) is the dye equilibrium concentration; K_L (L^3/mg) is a constant that related to the heat of adsorption; K_F (mg/g/(mg/L)^{3/n}) represents the adsorption capacity when C_{eq} equals 1; n represents the degree of dependence of adsorption on equilibrium concentration.

3 Results and discussion

3.1 FT-IR analyses

The FT-IR spectra of TiO₂ and PPy/TiO₂ are shown in Fig. 1. The intensity of the characteristic peak of hydroxyl group at 1630 cm^{-1} gradually decreases or even disappears as the rising of calcination temperature. This suggests that the amount of the hydroxyl group decreases with the increase of the calcination temperature. Furthermore, the intensities of the peaks at 1710 cm^{-1} , 1540 cm^{-1} and 1400 cm^{-1} corresponding to carboxyl group, anti-symmetric and symmetric stretching vibration of carboxylate group respectively, also reduce with increasing temperature [10]. Moreover, these peaks almost disappear when the temperature exceeds 350 °C. This result indicates that the citric acid molecules coordinated with TiO₂ are gradually decomposed with the increase of calcination temperature, which reduces the content of carboxyl and carbonyl groups on the surface of TiO₂. In addition, the intensity and shape of the peak at 400–800 cm^{-1} corresponding to Ti–O–Ti exhibit obvious changes with the increase of calcination temperature [16]. It is potentially due to the fact that the gradual disappearance of hydroxyl, carboxyl and carbonyl groups reduces the defects on the surface of TiO₂, which results in the formation of a certain crystal structure in TiO₂ [23]. It is obvious that the type and quantity of the

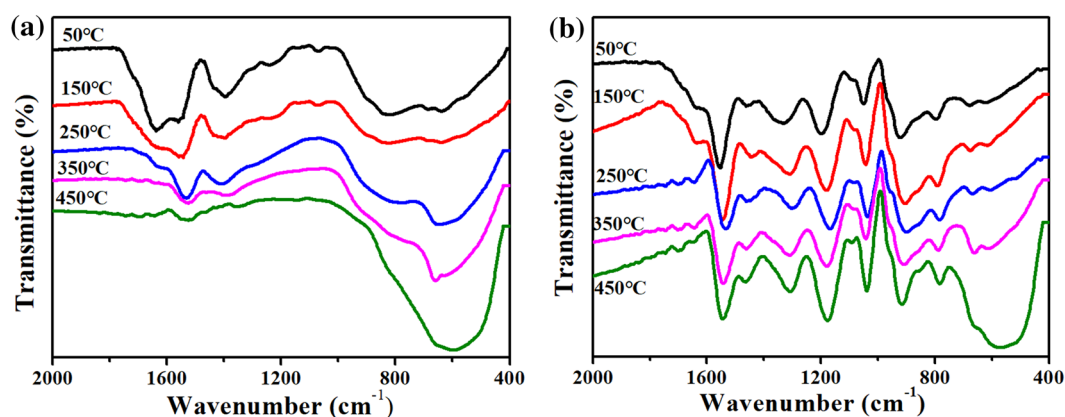


Fig. 1 FT-IR spectra of TiO₂ (a) and PPy/TiO₂ (b), respectively

Table 1 FT-IR adsorption bands of the PPy/TiO₂ composites and their assignments [3]

| 50-PPy/TiO ₂ | 150-PPy/TiO ₂ | 250-PPy/TiO ₂ | 350-PPy/TiO ₂ | 450-PPy/TiO ₂ | Assignment |
|------------------------------|--------------------------|--------------------------|--------------------------|--------------------------|--------------------------------------|
| Wave number/cm ⁻¹ | | | | | |
| 1554 | 1544 | 1533 | 1543 | 1543 | C=C stretching vibration |
| 1462 | 1444 | 1462 | 1462 | 1462 | C=N stretching vibration |
| 1331 | 1309 | 1302 | 1309 | 1309 | C-H or C-N in-plane deformation mode |
| 1200 | 1180 | 1169 | 1178 | 1176 | NH ⁺ deformation mode |

active functional groups on the surface of TiO₂ change with the calcination temperature, resulting in the variation of the surface chemical properties of TiO₂.

Figure 1b is the FT-IR spectra of the prepared PPy/TiO₂ composites, and the corresponding data are listed in Table 1. The positions of the bands related to PPy obviously change [17]. The band of Ti–O–i is not found in the spectra of 50-PPy/TiO₂, 150-PPy/TiO₂ and 250-PPy/TiO₂, but appears in that of 350-PPy/TiO₂ and 450-PPy/TiO₂. This may be because the active function groups on the surface of TiO₂ calcined at lower temperature can combine with PPy through strong chemical reaction. Therefore, the force between PPy and TiO₂ weakens with the increase of the calcination temperature due to the decrease of the active function groups.

3.2 TPD analyses

Figure 2 displays the TPD spectra of TiO₂ after calcination at different temperatures. The function groups on the surface of TiO₂ decompose upon heating and release CO and CO₂ at different temperatures, which can possibly be used to identify and estimate the active groups quantitatively. It has been reported that CO peaks result from the decomposition of the carbonyl groups at higher temperature, whereas CO₂ peaks derive from the decomposition of the carboxyl groups at low temperature [6, 19]. The TPD

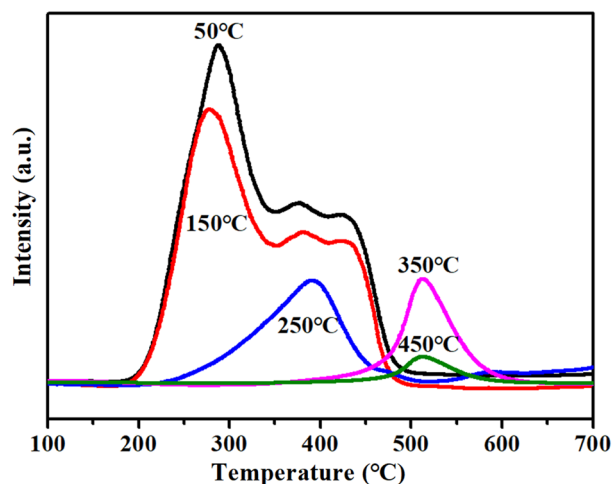


Fig. 2 TPD spectra of TiO₂ calcinated at different temperatures

spectra of 50-TiO₂ and 150-TiO₂ are basically similar, which are mainly CO₂ peak derived from the decomposition of carboxyl groups. However, the peak area of 150-TiO₂ is smaller than that of 50-TiO₂, suggesting that 150-TiO₂ possesses fewer carboxyl groups due to the high calcination temperature. For 250-TiO₂, the position and area of CO₂ peaks both change significantly, owing to the further decomposition of the function groups. The CO₂ peaks are replaced by CO peaks in the TPD spectra of 350-TiO₂ and

450-TiO₂ calcined at higher temperature, which implies that the carboxyl groups on the surface of TiO₂ are decomposed during the calcination progress, leaving only the carbonyl groups. In addition, considering 350-TiO₂ shows a larger peak area, 350-TiO₂ should contain more carbonyl groups than 450-TiO₂. Finally, the type and quantity of the function groups on the surface of TiO₂ have changed after calcination at different temperatures, resulting in the variation of the surface chemical properties.

3.3 XRD analyses

The XRD results of TiO₂ and PPy/TiO₂ are shown in Fig. 3. The crystal form of TiO₂ is transformed from amorphous to anatase as the calcination temperature rises [21, 24]. 350-TiO₂ exhibits anatase structure, and 450-TiO₂ displays a very clear anatase structure. According the previous FT-IR analyses, the decrease of the active function groups of TiO₂ calcined at higher temperature reduces the defects on the surface of TiO₂, which results in the formation of the crystal structure. It also can be seen that PPy/TiO₂ and TiO₂ at

the same temperature exhibit a similar crystal structure, although the peak intensities of PPy/TiO₂ are lower than that of pure TiO₂ due to the outer layer of PPy.

3.4 Zeta potentials

Figure 4 presents the zeta potentials of TiO₂ and PPy/TiO₂. The isoelectric point (pH_{iep}) is the pH value when the zeta potential value is zero. The pH_{iep} of 50-TiO₂, 150-TiO₂, 250-TiO₂, 350-TiO₂ and 450-TiO₂ are 2.27, 2.81, 4.65, 6.03 and 6.79, respectively, suggesting the pH_{iep} of TiO₂ increases with the calcination temperature, which is consistent with previous studies [20]. The reduction of the carboxyl groups on the TiO₂ surface promotes its electrical neutrality. However, the pH_{iep} of PPy/TiO₂ is larger than that of TiO₂. The pH_{iep} of 50-PPy/TiO₂, 150-PPy/TiO₂, 250-PPy/TiO₂, 350-PPy/TiO₂ and 450-PPy/TiO₂ are 2.73, 8.54, 9.80, 9.80 and 9.79, respectively, which are lower than that of pure PPy (pH_{iep} > 10) [4]. The distinction is related to the various content of carboxyl group on TiO₂ surface. When the content of carboxyl group is relatively high, it can involve into the

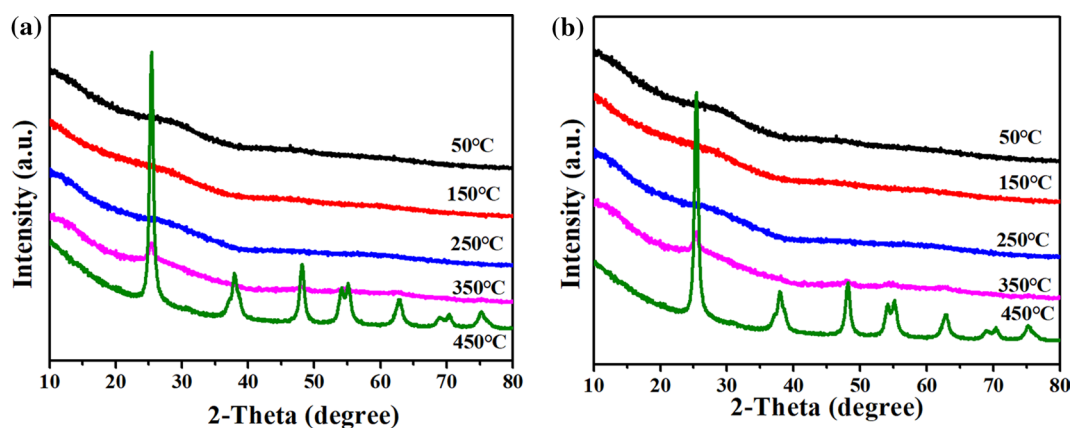


Fig. 3 XRD patterns of TiO₂ (a) and PPy/TiO₂ (b) at different calcination temperatures

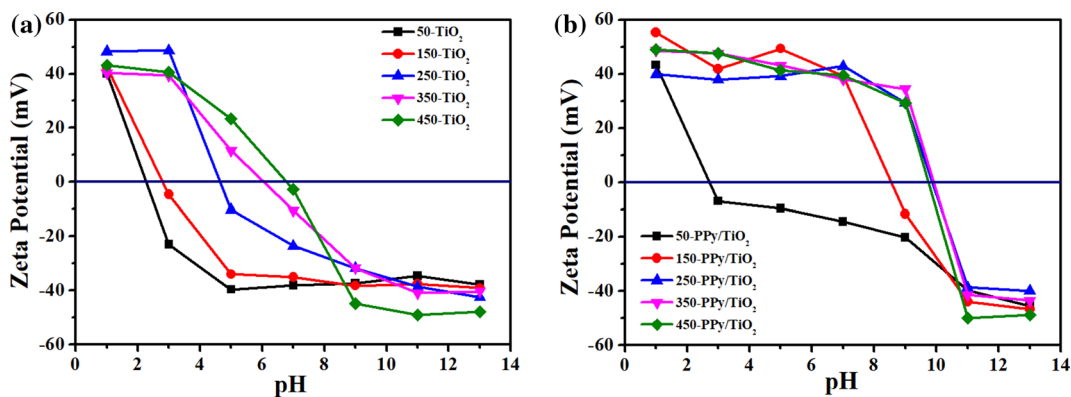


Fig. 4 Zeta potentials of TiO₂ (a) and PPy/TiO₂ (b) at different calcination temperatures

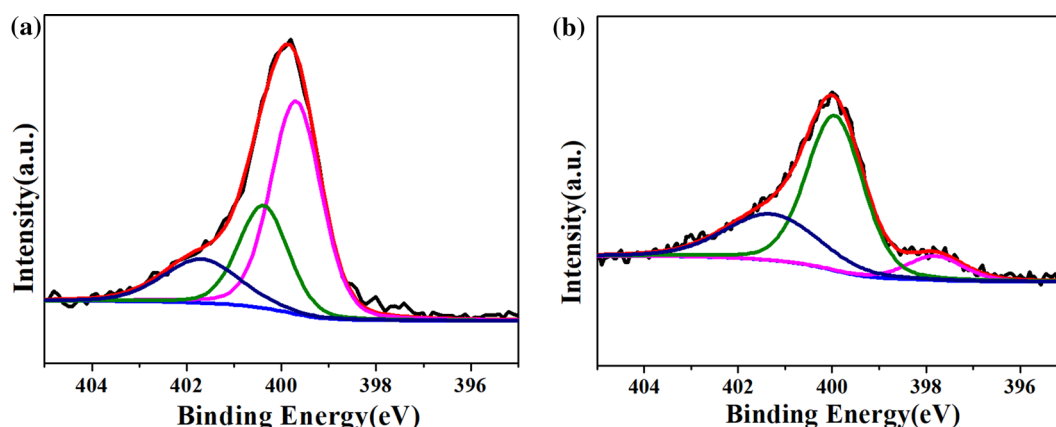


Fig. 5 XPS N1s core level spectra of the 50-PPy/TiO₂ (a) and 450-PPy/TiO₂ (b) composites

PPy chain and neutralize -NH^+ on the PPy chain, which make PPy/TiO₂ is negatively charged; while PPy/TiO₂ is positively charged when the carboxyl group is relatively low, which is not enough to neutralize all the -NH^+ groups [26]. This implies that the content of the carboxyl group on TiO₂ surface will impact the chemical properties of PPy/TiO₂.

3.5 XPS analyses

The XPS spectra of the 50-PPy/TiO₂ and 450-PPy/TiO₂ composites are displayed in Fig. 5. From the spectra, the peaks at 399.9 and 401.3 eV are attributed to the neutral nitrogen atoms (NH) and positively charged nitrogen atoms (N⁺) in PPy layer, respectively [11, 26]. The proportion of positively charged nitrogen atoms is found to be about 44% in terms of $[\text{N}^+]/[\text{N}]$. For 450-PPy/TiO₂, the peak at 397.4 eV attributed to the imine ($=\text{N}-$) structure appears in the spectrum instead of that at 402.1 eV ($=\text{N}^+-$). And its proportion of positively charged nitrogen atoms is about 29%. This suggests that 50-PPy/TiO₂ contains more positively charged nitrogen atoms, for the strong acidity of TiO₂ without calcination results in more nitrogen atoms of PPy to be protonated during the polymerization. Furthermore, it is obvious that 50-PPy/TiO₂ contains more oxygen atoms for the intensity ratio of N1 s and O1 s for 50-PPy/TiO₂ is larger than that of 450-PPy/TiO₂ (as shown in Fig. 6) which indicates the TiO₂ particles with many carboxyl groups can be dopants are inserted into the PPy chains [18, 25].

3.6 S_{BET} analyses

Besides, the specific surface areas of 50-TiO₂, 450-TiO₂, 50-PPy/TiO₂ and 450-PPy/TiO₂ are shown in Table 2. It is clear that the S_{BET} of 450-TiO₂ is larger than that of 50-TiO₂, it may be because high temperature calcination causes the organic matter on the surface of TiO₂ to

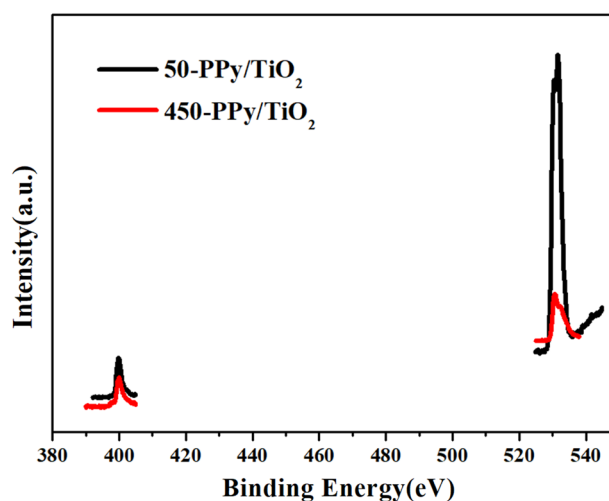


Fig. 6 XPS N1s and O1s core level spectra of the 50-PPy/TiO₂ and 450-PPy/TiO₂ composites

Table 2 Textural property of 50-TiO₂, 450-TiO₂, 50-PPy/TiO₂ and 450-PPy/TiO₂

| Samples | S _{BET} /m ² g ⁻¹ | V/cm ³ g ⁻¹ | R/nm |
|--------------------------|--|-----------------------------------|------|
| 50-TiO ₂ | 14.80 | 0.032 | 5.27 |
| 450-TiO ₂ | 87.92 | 0.17 | 6.83 |
| 50-PPy/TiO ₂ | 27.30 | 0.20 | 8.43 |
| 450-PPy/TiO ₂ | 85.66 | 0.098 | 5.83 |

decompose to produce more pore structure. In addition, the specific surface areas of PPy/TiO₂ and TiO₂ are similar, indicating that the introduction of polypyrrole does not cause significant changes in specific surface area. Similarly, the S_{BET} of 450-PPy/TiO₂ is larger than that of 50-PPy/TiO₂.

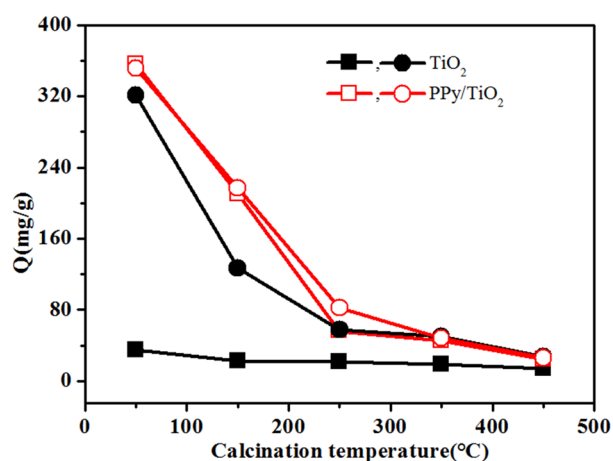


Fig. 7 Effects of calcination temperature on the adsorption capacities of TiO₂ and PPy/TiO₂ for ARG (square) and MB (roundness)

3.7 Adsorption performance

3.7.1 Effect of the calcination temperature

The prepared TiO₂ and PPy/TiO₂ are employed to adsorb ARG and MB (800 mg/L), and the results are shown in Fig. 7. The adsorption capacity of TiO₂ for ARG is much weaker than that for MB. This is because the carboxyl groups on the surface of TiO₂ generate electrostatic repulsion with ARG, but show electrostatic attraction with MB. In addition, the adsorption capacity declines dramatically as the calcination temperature increases. This is mainly attributed to the reduction of the adsorption sites, resulting from the decrease or even almost disappearance of carboxyl and hydroxyl groups on the surface of TiO₂ with the increase of calcination temperature.

However, PPy/TiO₂ exhibits an enhanced adsorption capacity for ARG and MB at the same condition. This is potentially because the neutralization of the carboxyl groups on the TiO₂ surface and $-NH^+$ on the PPy chain eliminates the repulsive force between the carboxyl groups and ARG. The oxygen atoms of PPy/TiO₂ can also be as the adsorption sites. The adsorption capacities of PPy/TiO₂ decrease with the increase of the calcination temperature. There are two potential reasons to elucidate the decrease of the adsorption capacity of PPy/TiO₂. One is the loss of adsorption active sites. The other is the weakened interaction between PPy and TiO₂ limits the delocalization of excess electrons from TiO₂ in the PPy chain, which decreases the dispersion effect between the outer layer PPy and the dye molecules, and ultimately reduces the adsorption capacity.

In addition, the adsorption capacities of 50-TiO₂ and 50-PPy/TiO₂ are higher than that of 450-TiO₂ and 450-PPy/TiO₂, although 450-TiO₂ and 450-PPy/TiO₂ have larger

specific surface areas (as shown in Table 2). This suggests that the specific surface area is not the main factor. The same conclusion has been confirmed in our published article [9].

3.7.2 Adsorption capacity of pure PPy

Furthermore, we also investigate the adsorption performance of pure PPy to further investigate the role of PPy on the adsorption capacity of PPy/TiO₂, as shown in Fig. 8. The concentrations of ARG and MB are both 300 mg/L. The adsorption capacity of pure PPy for MB is slightly higher than that for ARG. However, the adsorption capacity of pure PPy is not very well. It also finds that the adsorption capacity of PPy/TiO₂ is higher than the summation of the adsorption capacity of PPy and TiO₂. This may be because the formation of the covalent-like binding between PPy and TiO₂, followed by the increased N⁺ groups (as shown in Fig. 5), and then the enhanced capacity [13, 14].

3.7.3 Effects of pH and ionic concentration on adsorption

The adsorption performance of 50-PPy/TiO₂ is further investigated for its highest adsorption capacity. The influences of pH and ionic concentration of the dye solution on the adsorption capacity of 50-PPy/TiO₂ are shown in Fig. 9. The adsorption capacity of 50-PPy/TiO₂ for ARG decreases when pH is above 3, while that for MB rises with the increasing pH. The surface of 50-PPy/TiO₂ can be positively charged when pH is lower than pH_{iep} (2.73), and it can be negatively charged when pH is lower than pH_{iep} (2.73) [13, 14]. Therefore, anionic dye ARG can be adsorbed by positively charged 50-PPy/TiO₂ through

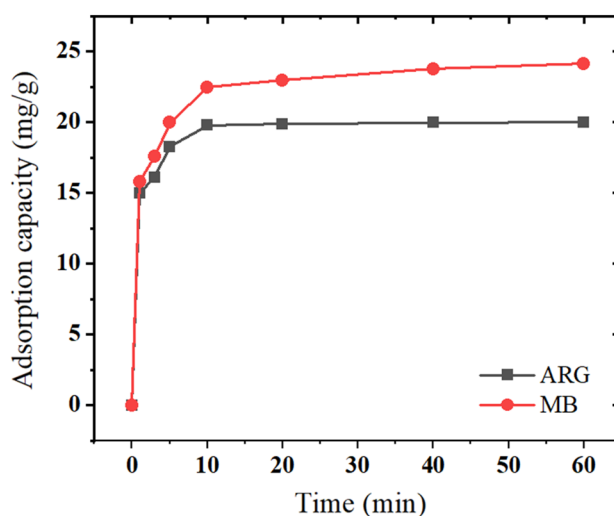


Fig. 8 The adsorption capacity of pure PPy for ARG and MB (300 mg/L)

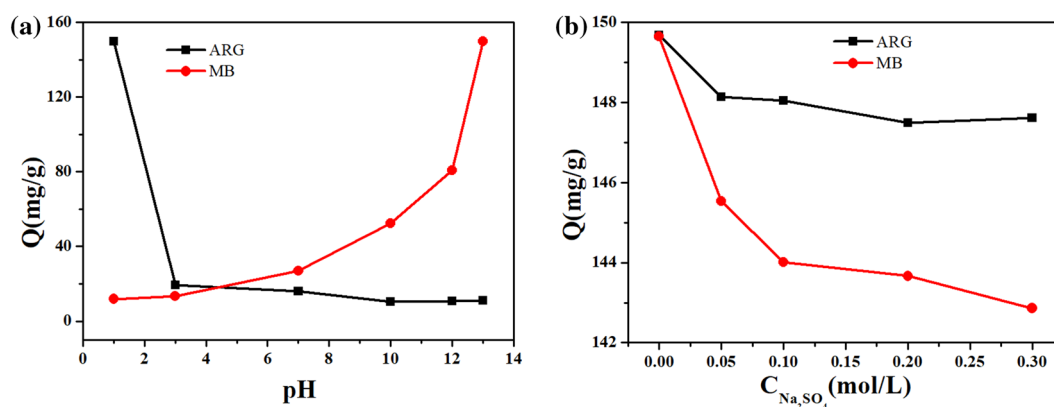


Fig. 9 Effects of pH (a) and ionic concentration (b) on the adsorption capacities of 50-PPy/TiO₂ for ARG and MB, respectively

the electrostatic attraction at a lower pH. Correspondingly, cationic dye MB can be adsorbed by negatively charged 50-PPy/TiO₂ through the electrostatic attraction at a higher pH. Besides, 50-PPy/TiO₂ still shows some adsorption capacity for ARG although the pH value is higher than 3, which means there maybe exists other adsorption forces except electrostatic effect, such as hydrogen bonding [8].

Besides, the effect of ionic concentration is also investigated, as shown in Fig. 8b. The result shows that the ionic concentration has a weak negative impact on the adsorption capacity of 50-PPy/TiO₂. Zhang et al. [25] indicated that the increase of ionic concentration reduced the electrostatic attraction between the adsorbates and adsorbents, and also reduced the electrostatic repulsion between the adsorbates. The former declined the adsorption capacity, and the latter improved it [15]. With the effects of these two aspects, the adsorption capacity of 50-PPy/TiO₂ is almost unchanged at the different ionic concentration.

3.7.4 Adsorption kinetics

It is essential that an adsorbent shows a rapid adsorption rate for the adsorbates. Figure 10 represents the influences of contact time and initial concentration on the adsorbed ARG and MB on 50-PPy/TiO₂, respectively. It is obvious that 50-PPy/TiO₂ can complete its adsorption process in a short contact time of 20 min. Therefore, it is feasible to choose 60 min as the adsorption time in the following adsorption experiments. Furthermore, 50-PPy/TiO₂ is still able to adsorb ARG and MB quickly even though the dye concentration is up to 800 mg/L, which suggests that 50-PPy/TiO₂ exhibits an excellent adsorption performance.

The fitting data of the adsorption kinetics of ARG and MB are listed in Table 3. The adsorption behavior of 50-PPy/TiO₂ can be well described by the pseudo-second-order model because the values of the correlation coefficients R^2 are close to 1. Furthermore, the calculated values of Q_{eq} from the pseudo-second-order model approximately equal to the experimental values. This indicated that the adsorption of

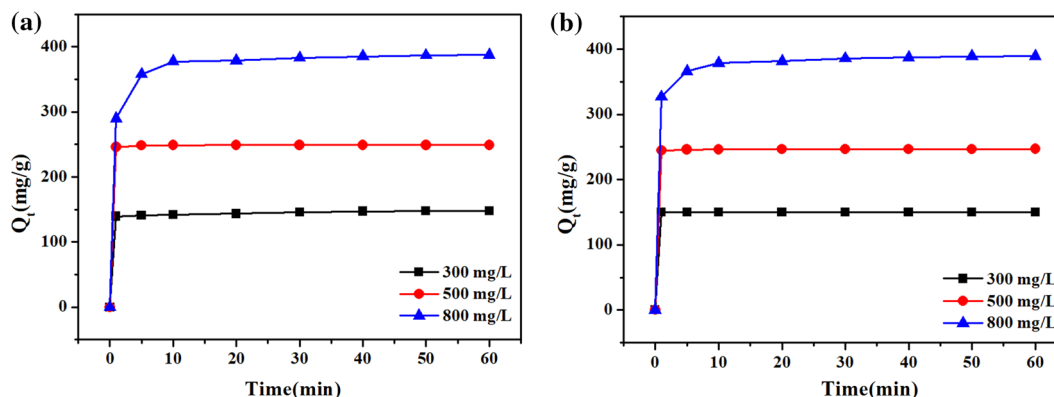
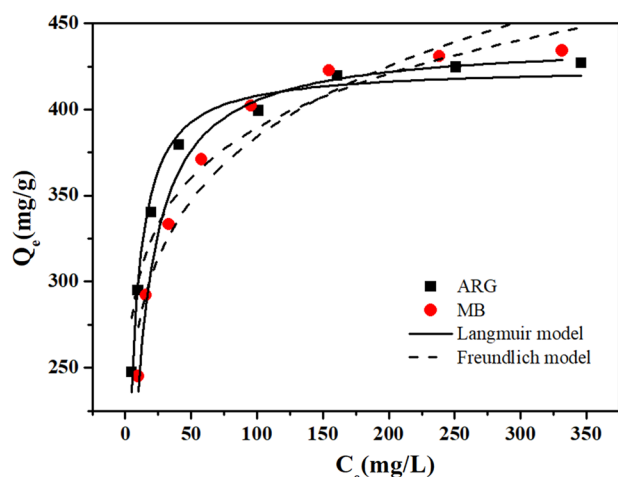


Fig. 10 Adsorption equilibrium curves of ARG and MB on PPy/TiO₂

Table 3 Kinetic parameters of ARG and MB adsorption on the 50-PPy/TiO₂ composite

| Dye | Concentration (mg/L) | First-order model | | | Second-order model | | |
|-----|----------------------|-------------------|-----------------|----------------|--------------------|-----------------|----------------|
| | | K ₁ | Q _{eq} | R ² | K ₂ | Q _{eq} | R ₂ |
| ARG | 300 | 0.091 | 23.42 | 0.7564 | 2.31 | 149.93 | 1.0 |
| | 500 | 0.16 | 3.29 | 0.5970 | 0.43 | 248.76 | 1.0 |
| | 800 | 0.11 | 95.29 | 0.8540 | 0.0060 | 389.10 | 0.9999 |
| MB | 300 | 0.0087 | 1.38 | 0.7212 | 1.72 | 149.93 | 1.0 |
| | 500 | 0.076 | 28.62 | 0.6605 | 0.14 | 246.91 | 1.0 |
| | 800 | 0.60 | 45.61 | 0.4556 | 0.0075 | 390.62 | 0.9999 |

**Fig. 11** Langmuir and Freundlich adsorption isotherm models of ARG and MB onto 50-PPy/TiO₂

ARG and MB on 50-PPy/TiO₂ is mainly attributed to chemisorption [13, 14].

3.7.5 Adsorption isotherm

Figure 11 represents the results of the adsorption isotherm which is employed to describe the interaction between 50-PPy/TiO₂ and dyes. The corresponding data are listed in Table 4. It is obvious that Langmuir isotherm model is more reasonable to describe the adsorption behavior of 50-PPy/TiO₂ for ARG and MB, for its higher correlation coefficient R². This means that the adsorption of ARG and MB onto 50-PPy/TiO₂ is the monolayer adsorption. Besides, the maximum adsorption capacities of ARG and MB are 424.75 and 439.61 mg/g, respectively, suggesting that 50-PPy/TiO₂ is an excellent adsorbent compared with activated carbon.

Table 4 Parameters of Langmuir and Freundlich adsorption isotherm models

| Dye | Langmuir model | | | | Freundlich model | | |
|-----|------------------|----------------|----------------|----------------|------------------|------|----------------|
| | Q _{max} | K _L | R ² | R _L | K _F | 1/n | R ² |
| ARG | 424.75 | 0.24 | 0.9810 | 0.0035 | 232.36 | 0.11 | 0.8992 |
| MB | 439.61 | 0.12 | 0.9777 | 0.0069 | 195.85 | 0.15 | 0.9221 |

The dimensionless separation factor, R_L , which is an essential characteristic of the Langmuir model to define the favorability of an adsorption process, is expressed as

$$R_L = \frac{1}{1 + K_L C_m} \quad (7)$$

where C_m is the maximum initial concentration of ARG and MB (1200 mg/L). The calculated R_L values are 0.0035 and 0.0069 for the adsorption of ARG and MB, respectively, which are in the range of 0–1, indicating the adsorption process is favorable.

4 Conclusion

In this article, the PPy/TiO₂ composites synthesized by polymerizing pyrrole monomer on the surface of TiO₂ calcined at different temperatures were employed to adsorb ARG and MB. The results of FT-IR, XRD, TPD and Zeta potentials indicated that the functional groups (hydroxyl and carboxyl groups) of TiO₂ decreased with the increase of calcination temperature. This led to the gradual decrease of the adsorption capacity of TiO₂. The results of FT-IR, XRD, Zeta potentials and XPS further suggested that the chemical properties of TiO₂ had a strong impact on that of PPy/TiO₂. The force between the inner TiO₂ and outer PPy of the PPy/TiO₂ composites was weakened when the TiO₂ particles were calcined at higher temperature. The adsorption capacity of PPy/TiO₂ was the strongest when TiO₂ was not calcined, and gradually decreased with the increase of the calcination temperature of TiO₂. The result of the effect of pH suggested that ARG could be adsorbed by PPy/TiO₂ under acidic condition, and MB could be adsorbed by PPy/TiO₂ under alkaline condition. Besides, the ionic concentration had a negative effect on the adsorption performance of PPy/TiO₂. The equilibrium adsorption of ARG and MB on PPy/TiO₂.

TiO₂ was achieved in a short time of 20 min. Its adsorption kinetics was well described by the pseudo-second-order model. The Langmuir isotherm model was found for PPy/TiO₂ with the maximum adsorption amount of 424.75 and 439.61 mg/g for ARG and MB, respectively. Finally, the surface chemical properties of TiO₂ had a great influence on the adsorption performance of the synthesized PPy/TiO₂. The PPy/TiO₂ composite could possess excellent adsorption performance when the selected TiO₂ contained more hydroxyl and carboxyl groups.

Compliance with ethical standards

Conflict of interest The authors declare that they have no competing interests.

References

1. Ballav N, Maity A, Mishra SB (2012) Highly efficient removal of chromium(VI) using glycine doped polypyrrole adsorbent from aqueous solution. *Chem Eng J* 198–199(4):536–546
2. Bhaumik M, Maity A, Srinivasu VV, Onyango MS (2011) Enhanced removal of Cr(VI) from aqueous solution using polypyrrole/Fe₃O₄ magnetic nanocomposite. *J Hazard Mater* 190(1):381–390
3. Blinova NV, Stejskala J, Prokeš J, Omastová M (2007) Polyaniline and polypyrrole: a comparative study of the preparation. *Eur Polym J* 43(6):2331–2341
4. Cassignol C, Olivier P, Ricard A (2015) Influence of the dopant on the polypyrrole moisture content: effects on conductivity and thermal stability. *J Appl Polym Sci* 70(8):1567–1577
5. Chen J, Feng JT, Yan W (2016) Influence of metal oxides on the adsorption characteristic of PPy/metal oxides for methylene blue. *J Colloid Interf Sci* 475:26–35
6. Faria PCC, Órfão JJM, Pereira MFR (2004) Adsorption of anionic and cationic dyes on activated carbons with different surface chemistries. *Water Res* 38(8):2043–2052
7. Feng J, Li J, Lv W, Xu H, Yang H, Yan W (2014) Synthesis of polypyrrole nano-fibers with hierarchical structure and its adsorption property of Acid Red G from aqueous solution. *Synth Met* 191(9):66–73
8. Feng J, Chen J, Wang N, Li J, Shi J, Yan W (2016) Enhanced adsorption capacity of polypyrrole/TiO₂ composite modified by carboxylic acid with hydroxyl group. *RSC Adv* 6(48):42572–42580
9. Feng J, Zhu J, Lv W et al (2015) Effect of hydroxyl group of carboxylic acids on the adsorption of Acid Red G and Methylene Blue on TiO₂. *Chem Eng J* 269:316–322
10. Janković IA, Šaponjić ZV, Čomor MI, Nedeljković JM (2009) Surface modification of colloidal TiO₂ nanoparticles with bidentate benzene derivatives. *J Phys Chem C* 113(29):12645–12652
11. Kang ET, Neoh KG, Ong YK, Tan KL, Tan BTG (1991) X-ray photoelectron spectroscopic studies of polypyrrole synthesized with oxidative iron(III) salts. *Macromolecules* 24(10):2822–2828
12. Karthikeyan M, Satheeshkumar KK, Elango KP (2009) Removal of fluoride ions from aqueous solution by conducting polypyrrole. *J Hazard Mater* 167(1):300–305
13. Li J, Feng J, Yan W (2013) Excellent adsorption and desorption characteristics of polypyrrole/TiO₂ composite for Methylene Blue. *Appl Surf Sci* 279(8):400–408
14. Li J, Zhang Q, Feng J, Yan W (2013) Synthesis of PPy-modified TiO₂ composite in H₂SO₄ solution and its novel adsorption characteristics for organic dyes. *Chem Eng J* 225(4):766–775
15. Li W, Lin Q, Gao M, Ma H (2017) Adsorption studies of orange II onto polyaniline/bentonite nanocomposite. *Water Sci Technol* 76(2):337–354
16. Li X, Wang D, Cheng G, Luo Q, An J, Wang Y (2008) Preparation of polyaniline-modified TiO₂ nanoparticles and their photocatalytic activity under visible light illumination. *Appl Catal B Environ* 81(3):267–273
17. Lim CW, Song K, Kim SH (2012) Synthesis of PPy/silica nanocomposites with cratered surfaces and their application in heavy metal extraction. *J Ind Eng Chem* 18(1):24–28
18. Myers RE (1986) Chemical oxidative polymerization as a synthetic route to electrically conducting polypyrroles. *J Electron Mater* 15(2):61–69
19. Órfão JJM, Silva AIM, Pereira JCV, Barata SA, Fonseca IM, Faria PCC, Pereira MFR (2006) Adsorption of a reactive dye on chemically modified activated carbons—influence of pH. *J. Colloid Interf Sci* 296(2):480–489
20. Siviglia P, Daggetti A, Trasatti S (1983) Influence of the preparation temperature of ruthenium dioxide on its point of zero charge. *Colloid Surface* 7(1):15–27
21. Tang Z, Zhang J, Cheng Z, Zhang Z (2003) Synthesis of nano-sized rutile TiO₂ powder at low temperature. *Mater Chem Phys* 77(2):314–317
22. Weidlich C, Mangold KM, Jüttner K (2005) Continuous ion exchange process based on polypyrrole as an electrochemically switchable ion exchanger. *Electrochim Acta* 50(25):5247–5254
23. Wu R, Qu J, He H, Yu Y (2004) Removal of azo-dye Acid Red B (ARB) by adsorption and catalytic combustion using magnetic CuFe₂O₄ powder. *Appl Catal B-Environ* 48(1):49–56
24. Yu JG, Yu HG, Cheng B, Zhao XJ, Yu JG, Ho WK (2003) The effect of calcination temperature on the surface microstructure and photocatalytic activity of TiO₂ thin films prepared by liquid phase deposition. *J Phys Chem B* 107(50):13871–13879
25. Zhang X, Bai R (2002) Adsorption behavior of humic acid onto polypyrrole-coated nylon 6,6 granules. *J Mater Chem* 12(9):2733–2739
26. Zhang X, Bai R (2003) Surface electric properties of polypyrrole in aqueous solutions. *Langmuir* 19(26):10703–10709

Publisher's Note Springer Nature remains neutral with regard to jurisdictional claims in published maps and institutional affiliations.